Binding of Neuroligins to PSD-95

M. Irie, Y. Hata, M. Takeuchi, K. Ichtchenko, A. Toyoda, K. Hirao, Y. Takai, T. W. Rosahl, T. C. Südhof*

PSD-95 is a component of postsynaptic densities in central synapses. It contains three PDZ domains that localize *N*-methyl-D-aspartate receptor subunit 2 (NMDA2 receptor) and K^+ channels to synapses. In mouse forebrain, PSD-95 bound to the cytoplasmic COOH-termini of neuroligins, which are neuronal cell adhesion molecules that interact with β-neurexins and form intercellular junctions. Neuroligins bind to the third PDZ domain of PSD-95, whereas NMDA2 receptors and K^+ channels interact with the first and second PDZ domains. Thus different PDZ domains of PSD-95 are specialized for distinct functions. PSD-95 may recruit ion channels and neurotransmitter receptors to intercellular junctions formed between neurons by neuroligins and β-neurexins.

Synapses are asymmetric junctions between neurons that transfer signals from a presynaptic neuron to a postsynaptic cell. A family of plasma membrane proteins called PSD-95/SAP90, PSD-93/chapsyn, SAP102, and SAP97/hDLG is present at synaptic junctions (*1*). These proteins are similar to proteins from other intercellular junctions (ZO-1/-2 from tight junctions, dlg-A from septate junctions) (*2*). All these proteins are composed of three NH_2-terminal PDZ domains, a single interior SH3 domain, and a COOH-terminal guanylate kinase domain that is enzymatically inactive. The PDZ domains of PSD-95 and related proteins interact with the COOH-terminal sequences of K^+ channels and NMDA2 receptors (*3*). By these interactions, PSD-95 may mediate the clustering of K^+ channels and NMDA receptors at synapses. It remains unknown, however, how PSD-95 is recruited to synaptic junctions.

Neuroligins are neuronal cell-surface proteins composed of an extracellular domain that resembles acetylcholinesterase, a transmembrane domain, and a highly conserved intracellular sequence (*4*). The extracellular domain of neuroligins tightly binds to the extracellular domain of β-neurexins, which are also cell-surface proteins (*5*). Only a differentially spliced subset of β-neurexins binds to neuroligins. Neurexins and neuroligins are detectable only in neurons where they are enriched in synaptic plasma membranes (*4*, *5*). Neuroligins and β-neurexins localized on separate cells bind to each other and form a heterotypic intercellular junction regulated by alternative splicing (*6*). We quantified the concentrations of neurexin and neuroligin mRNAs in mouse brain during postnatal development to determine their developmental profile (*7*). We used total RNA prepared from forebrain and PhosphorImager quantification of Northern blot signals and normalized all mRNA signals for the amounts of glyceraldehyde phosphate dehydrogenase (GAPDH). These analyses revealed a coordinate postnatal increase in the amounts of neurexin and neuroligin mRNAs with peak expression between postnatal days 5 and 10. Thereafter, the mRNAs declined to a constant concentration of 25 to 40% of the peak quantities (not shown). By comparison, analysis of expression of GAP-43, a protein implicated in axonal pathfinding, also revealed a postnatal peak of expression; however, this peak of expression was earlier than that observed for neurexins and neuroligins. No peak was observed for a series of control mRNAs. These data suggest a developmentally late function for the β-neurexin–neuroligin junction that operates in mature neurons.

To gain insight into the intracellular anchoring mechanism for this junction, we have searched for binding proteins for the cytoplasmic domain of neuroligins. We used yeast two-hybrid selection and screened a prey cDNA library from rat brain with a bait plasmid encoding the cytoplasmic tail of neuroligin 2 (*8*). Sixteen isolates were obtained, two of which encoded PDZ domains from PSD-95. Retransformation of fresh yeast cells confirmed that these clones specifically interacted and were the most strongly reactive among the specific clones isolated. To test whether the cytoplasmic domains of other neuroligins also interact with PSD-95, and whether isoforms of PSD-95 also bind to neuroligins, we quantified the yeast two-hybrid interactions by measuring β-galactosidase transactivation (Table 1). For this purpose, isoforms of PSD-95 were cloned first by polymerase chain reaction (PCR) and then by standard cDNA cloning techniques; then they were inserted into the appropriate yeast two-hybrid vectors (*9*). The cytoplasmic domains of all three neuroligins interacted with the NH_2-terminus of PSD-95, which contains the three PDZ domains. Furthermore, the NH_2-terminal fragments of the PSD-95 homologs PSD-93 and SAP102 (also containing three PDZ domains) were also strongly active. The strength of the interaction was similar for the different neuroligins and was comparable to that observed with the intracellular domains of NMDA receptors and the K^+ channel (Table 1). In contrast, we observed no interaction of any of these proteins with the NH_2-terminal three PDZ domains of ZO-1, a tight junction protein, or with the PDZ domains of dlg-A or nitric oxide synthase. Thus there appears to be a specific interaction of all three neuroligins with the PDZ domains of three distinct but related synaptic proteins—PSD-95, PSD-93, and SAP102.

The first and second, but not the third, PDZ domains of PSD-95, bind tightly to the cytoplasmic COOH-termini of NMDA receptors and K^+ channels, which suggests that the three PDZ domains of PSD-95 are not equivalent (*3*). We therefore used yeast two-hybrid assays to investigate the ability of individual PDZ domains from PSD-95 to bind to neuroligins, K^+ channels, and NMDA receptors (Table 1). The first and second PDZ domains alone bound only weakly to the cytoplasmic tail of neuroligins; in combination, binding was much stronger. These two PDZ domains, however, interacted strongly with NMDA receptors and K^+ channels. In contrast, neuroli-

Structures of encoded cytoplasmic domains	Bait plasmid	β-Galactosidase activity
	pBTM116 NL1-1	1451 ± 24
	pBTM116 NL1-2	<20
	pBTM116 NL1-5	<20
	pBTM116 NL1-6	737 ± 4
	pBTM116 NL1-10	2400 ± 4
	pBTM116 NL2-1	896 ± 48
	pBTM116 NL2-2	<20
	pBTM116 NL2-3	1923 ± 16

Fig. 1. Sequence dependence of neuroligin interaction with PSD-95. Parts of cytoplasmic tails of neuroligins that were deleted are indicated as hatched regions. β-Galactosidase activities are given in nanomoles per minute per milligram of protein (*8*, *9*).

M. Irie, M. Takeuchi, A. Toyoda, K. Hirao, Takai Biotimer Project, ERATO, Japan Science and Technology Corporation, 2-2-10, Murotani, Nishi-ku, Kobe, 651-22, Japan. Y. Hata, Howard Hughes Medical Institute and Department of Molecular Genetics, University of Texas Southwestern Medical Center at Dallas, Dallas, TX 75235–9050, USA, and Takai Biotimer Project, ERATO, Japan Science and Technology Corporation, 2-2-10, Murotani, Nishi-ku, Kobe 651-22, Japan.
K. Ichtchenko, T. W. Rosahl, T. C. Südhof, Howard Hughes Medical Institute and Department of Molecular Genetics, University of Texas Southwestern Medical Center at Dallas, Dallas, TX 75235–9050, USA.
Y. Takai, Takai Biotimer Project ERATO, Japan Science and Technology Corporation, 2-2-10, Murotani, Nishi-ku, Kobe 651-22, Japan, and Department of Molecular Biology and Biochemistry, Osaka University Medical School, Suita 565, Japan.
*To whom correspondence should be addressed.

Table 1. Interactions between the cytoplasmic domains of neuroligins and various PDZ domains. Data list β-galactosidase activities of yeast strains harboring the respective bait and prey plasmids. Single colonies from yeast cotransformed with the listed prey and bait vectors were selected on plates supplemented with minimal medium that lacked uracil, tryptophan, and leucine and were grown in liquid culture in the presence of selection medium for 40 hours. β-Galactosidase activity and protein concentrations of cell extracts were determined in triplicate (*8*). Data shown are nanomoles of substrate hydrolyzed per minute per milligram of protein ± SD after background subtraction; —, not tested; <20, no detectable activity. For plasmids, see (*9*).

Prey vector		Bait vector (in pBTM116)						
		NL1-1	NL1-10	NL2-1	NL3	NMDAR2A	NMDAR2B	Shaker
PSD-95								
pVP16PSD95-2	(PDZ 1–3)	1437 ± 24	453 ± 10	2635 ± 48	1350 ± 6	3303 ± 159	2875 ± 113	2481 ± 263
pVP16SAP90-5	(PDZ 1)	46 ± 2	—	—	—	2460 ± 33	—	328 ± 30
pVP16SAP90-6	(PDZ 2)	34 ± 0	—	—	—	639 ± 23	—	256 ± 3
pPrey514	(PDZ 3)	2068 ± 340	859 ± 32	466 ± 0	1809 ± 156	<20	<20	<20
SAP102								
pVP16SAP102-1	(PDZ 1–3)	885 ± 7	1046 ± 5	720 ± 13	789 ± 6	2988 ± 241	4600 ± 396	4254 ± 428
PSD-93								
pVP16PSD93-1	(PDZ 1–3)	1394 ± 55	428 ± 18	596 ± 76	566 ± 10	3311 ± 100	2883 ± 231	3147 ± 67
ZO-1								
pVP16ZO1-1	(PDZ 1–3)	<20	—	<20	<20	<20	—	—
DLG1								
pVP16dlg-1	(PDZ 1–3)	<20	—	<20	<20	82 ± 12	—	—
NOS								
pVP16NOS	(PDZ 1)	<20	—	<20	<20	<20	—	—

gins interacted strongly with the third PDZ domain of PSD-95, which exhibited no detectable binding to NMDA receptors and K^+ channels as described (*3*). Thus the three PDZ domains of PSD-95 are specialized for different interactions; the first two PDZ domains bind NMDA receptors and K^+ channels, whereas the third PDZ domain is specific for neuroligins.

A COOH-terminal sequence motif in the NMDA2 receptor and K^+ channels (Thr/Ser-Xaa-Val, where Xaa is any amino acid) is required for binding to the first and second PDZ domains of PSD-95 (*3*). As revealed by the crystal structure (*10*), the third PDZ domain of PSD-95 also binds a COOH-terminal Thr/Ser-Xaa-Val sequence, although the ligand for this PDZ domain was not known. The COOH-terminal region of all neuroligins contains the sequence His-Ser-Thr-Thr-Arg-Val, which conforms to the binding motif. This suggests that neuroligins may bind to the third PDZ domain of PSD-95 via their COOH-terminus. We tested this hypothesis with deletion constructs in yeast two-hybrid assays (Fig. 1). The COOH-terminal 48 residues from neuroligin 1 were sufficient for binding to PSD-95. Deletion of only three COOH-terminal amino acids (Thr-Arg-Val) abolished binding, which indicates that the interaction depends on the

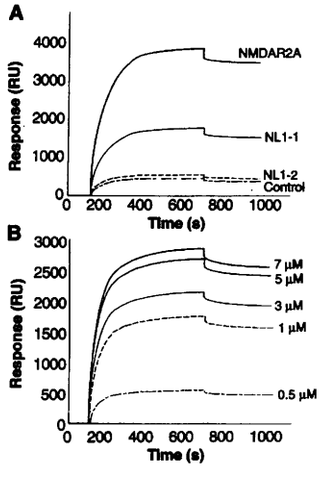

Fig. 2. Plasmon resonance analysis of interaction of PSD-95 with neuroligin 1 and NMDA receptor. (**A**) Synthetic peptides from the COOH-terminus of the NMDA2A receptor (NMDAR2A), neuroligin 1 (NL1-1), neuroligin 1 with a deletion of the last three residues (NL1-2), or a control peptide ending with a Thr-Ser-Val sequence (control) were immobilized on a BIACore CM5 sensor chip (*11*). Sensorgrams were recorded in real time during superfusion of 5 μM GST fusion protein containing the three PDZ domains of PSD-95. (**B**) Reaction of immobilized full-length neuroligin 1 peptide with the indicated concentrations of the PSD-95 GST fusion protein to determine binding affinity. Similar experiments were performed for the NMDA2A receptor peptide (not shown). RU, resonance units.

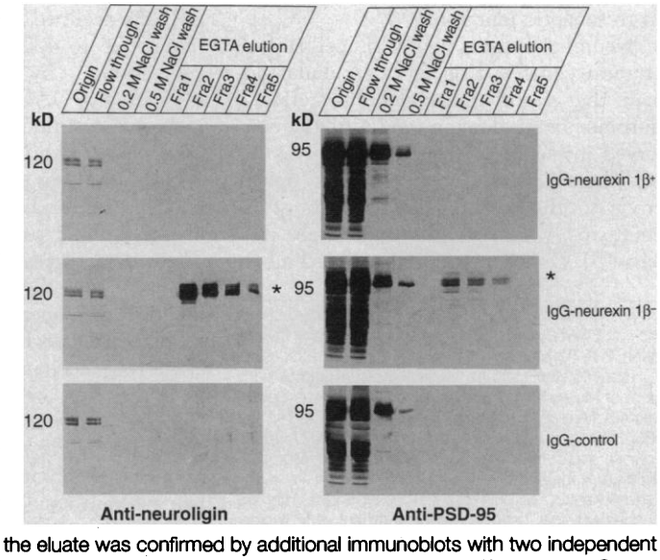

Fig. 3. Copurification of PSD-95 with neuroligins on immobilized neurexin 1β. Three recombinant fusion proteins containing a COOH-terminal IgG domain fused to the following NH_2-terminal sequences were used: IgG–neurexin $1\beta^+$, neurexin 1β with an insert in splice site 4; IgG–neurexin $1\beta^-$, neurexin 1β without an insert at splice site 4; IgG-control, a short NH_2-terminal control sequence. Affinity chromatography fractions obtained with immobilized IgG fusion proteins were blotted with polyclonal antibodies to neuroligins (left) and to PSD-95 (right). Identification of PSD-95 in the eluate was confirmed by additional immunoblots with two independent monoclonal antibodies to PSD-95, one of which was obtained from M. B. Kennedy (not shown). Strong reactivity with the PSD-95 antibody of multiple low bands in the origin and flow-through lanes (right) is caused by rapid proteolysis of PSD-95 in brain homogenates after solubilization; these bands are not visible when preimmune serum or monoclonal antibodies are used and are not due to nonspecific crossreactivity. Asterisks identify neuroligin and PSD-95 coeluting only from the IgG–neurexin $1\beta^-$ column.

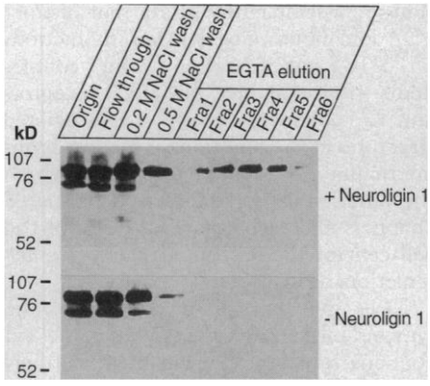

Fig. 4. Neuroligin is required for binding of PSD-95 to immobilized neurexin 1β⁻. Extracts from COS cells transfected with PSD-95 were mixed with extracts from COS cells transfected with a neuroligin 1 plasmid (top) or a control plasmid (bottom) and then subjected to affinity chromatography on immobilized IgG-neurexin 1β⁻. Fractions were immunoblotted for PSD-95. Numbers on the left indicate positions of size markers.

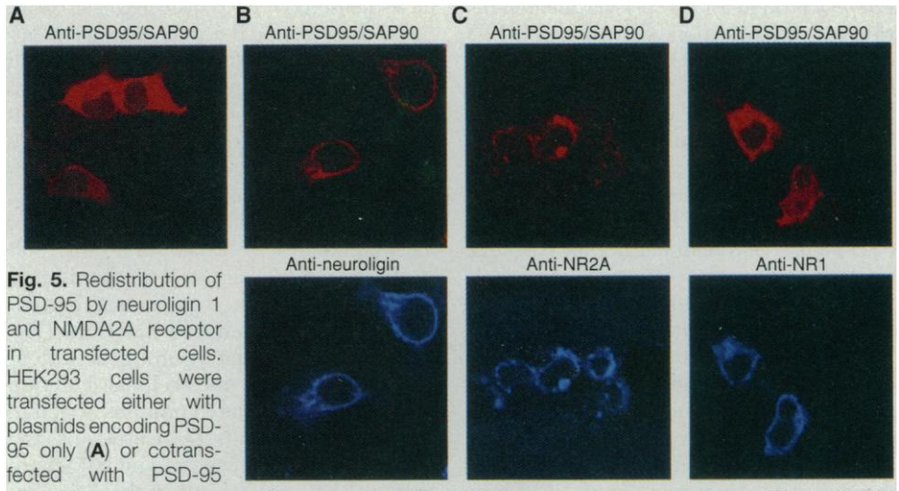

Fig. 5. Redistribution of PSD-95 by neuroligin 1 and NMDA2A receptor in transfected cells. HEK293 cells were transfected either with plasmids encoding PSD-95 only (**A**) or cotransfected with PSD-95 plasmids and plasmids encoding neuroligin 1 (**B**), NMDA2A type glutamate receptors (**C**), or NMDA1 type glutamate receptors (**D**) (*13*). Cells were immunostained for PSD-95 (top row) and the respective cotransfected proteins (bottom row) and visualized in a confocal microscope.

COOH-terminus of neuroligins.

Because yeast two-hybrid assays are prone to artifacts and do not allow an assessment of binding affinities, we analyzed the binding of neuroligins to PSD-95 directly by surface plasmon resonance (*11*). We immobilized four peptides on BIAcore sensor chips: a peptide containing the COOH-terminal 16 residues of neuroligin 1 (NL1-1), the same peptide lacking the last three amino acids (NL1-2, negative control), a peptide containing the COOH-terminal 16 residues of the NMDA2 receptor (NMDAR2A), and a second negative control with a 17-residue peptide that also ends with a Thr-Xaa-Val motif from the interior sequence of PSD-95. Superfusion of the immobilized peptides with a glutathione-S-transferase (GST) fusion protein from PSD-95 that contained all three PDZ domains resulted in a strong signal for the NMDA receptor and the wild-type neuroligin peptides but not for the truncated neuroligin peptide or the second control peptide (Fig. 2A). Superfusion with a GST fusion protein that contained the COOH-terminal domains of PSD-95 (SH3 and guanylate kinase domains) failed to elicit a binding signal (not shown). Thus the binding reaction is specific to the PDZ domains of PSD-95 and requires the COOH-terminal three amino acids of neuroligin. Binding does not occur with any Thr-Xaa-Val sequence because the control peptide from the interior PSD-95 sequence did not interact. Analysis of the binding affinity with a series of concentrations of GST fusion protein allowed us to estimate the affinity under our assay conditions ($K_M \approx 2.3 \pm 0.4 \times 10^{-7}$ M for neuroligin 1; $K_M \approx 2.1 \pm 0.4 \times 10^{-7}$ M for the NMDA2 receptor) (Fig. 2B and not shown). These data suggest that the COOH-terminus of neuroligin 1 directly interacts with the PDZ domains of PSD-95 and that the specificity of the interaction is determined by other sequence elements in addition to the COOH-terminal Thr/Ser-Xaa-Val motif.

To investigate whether neuroligins are present in a complex with PSD-95 in vivo, we purified neuroligins from brain homogenates by affinity chromatography on immobilized β-neurexin and tested whether neuroligins are complexed with PSD-95. Recombinant neurexin 1β was produced as a fusion protein with the COOH-terminus of immunoglobulin G (IgG), either without (1β⁻) or with (1β⁺) an insert in splice site 4, the splice site that regulates neuroligin binding (*4*). We then immobilized the recombinant neurexins and a control IgG protein and performed calcium-dependent affinity chromatography experiments with total brain homogenates on the immobilized protein columns (*12*). Immunoblotting of the chromatography fractions revealed that neuroligins were purified on the neurexin 1β⁻ column but not on the neurexin 1β⁺ or the control IgG columns (Fig. 3, left). PSD-95 was present only in the fractions that contained neuroligins, which suggests that neuroligins and PSD-95 are present in a complex in native brain (Fig. 3, right). Identification of the 95-kD band in the column eluates as PSD-95 was confirmed by additional immunoblots with two independent monoclonal antibodies to PSD-95 (not shown). Binding of neuroligins to the column is stronger than that of PSD-95, which is not surprising in view of the tightness of the neurexin-neuroligin interaction and the relatively high off-rates of interactions mediated by PDZ domains.

Although the data in Fig. 3 suggest that at least part of PSD-95 in brain homogenates is present in a complex with neuroligins, alternative explanations are that PSD-95 binds to neurexin 1β⁻ instead of neuroligins or that a second bridging protein in brain mediates the interaction of PSD-95 with neuroligins or neurexin 1β⁻. To rule out these possibilities, we applied proteins from COS cells that expressed full-length PSD-95 to a neurexin 1β⁻ column in the presence or absence of extracts from COS cells that expressed neuroligin 1. Binding of PSD-95 to the columns was observed only in the presence of neuroligin 1, which confirms that PSD-95 binding to the column requires neuroligin but not other brain proteins (Fig. 4).

To eliminate the possibility that the interaction of PSD-95 with neuroligins occurs only in vitro or after homogenization, we investigated whether PSD-95 binds to neuroligins in vivo by imaging the localization of PSD-95, neuroligins, and the NMDA2 receptor in transfected 293 cells (*13*). Cells that express only PSD-95 exhibit a diffuse cytoplasmic distribution of PSD-95 (Fig. 5A). Cotransfection of either neuroligin 1 or the NMDA2 receptor with PSD-95 changed this picture; PSD-95 became colocalized with neuroligin 1 or the NMDA2 receptor on the plasma membrane (Fig. 5, B and C), which suggests that PSD-95 is recruited to the plasma membrane by neuroligin 1 or NMDA2 receptors. By contrast, cotransfection of PSD-95 with NMDA1 receptors did not lead to recruitment of PSD-95 to plasma membranes (Fig. 5D). Cotransfection of neuroligin with a PSD-95 construct with only the first two PDZ domains did not result in recruitment of the

PSD-95 protein to the plasma membrane, whereas cotransfection of the same PSD-95 construct with NMDA2 receptor localized the PSD-95 protein to the membrane (data not shown). Thus neuroligin and the NMDA2 receptor cause a specific redistribution of PSD-95 in a living cell from the cytosol to the plasma membrane in a manner that requires the third PDZ domain of PSD-95 for neuroligin but not for NMDA2 receptors.

Our data indicate that neuroligins physiologically interact with PSD-95. This conclusion is supported by the following findings: (i) All three neuroligins specifically interact with three members of the PSD-95 family in yeast two-hybrid assays. (ii) The interactions require the COOH-terminal three amino acids of neuroligins. (iii) These interactions are mediated by the third PDZ domain, which does not bind to other known ligands of PDZ domains. (iv) A neuroligin–PSD-95 complex can be purified from native brain homogenates. (v) Binding can be reconstituted when PSD-95 and neuroligin 1 are separately expressed in COS cells. (vi) In transfected 293 cells, PSD-95 is recruited to the plasma membrane by neuroligin 1. (vii) Neuroligins and PSD-95 are copurified with synaptic junctions in subcellular fractionation experiments (*4*). The binding of neuroligins as cell adhesion molecules to PSD-95 establishes a link between intercellular junction formation and channel and receptor localization.

These results suggest a mechanism by which PDZ domain proteins may participate in neuronal cell–cell junctions (Fig. 6). We propose that neuroligins and β-neurexins form an intercellular junction (*6*). PSD-95 and related proteins attach to the cytoplasmic tails of neuroligins and recruit NMDA2 receptors and K^+ channels to the neuroligin side of this junction. On the neurexin side of the junction, the cytoplasmic COOH-termini of neurexins interact with a different PDZ domain protein called CASK (*14*). CASK is also related to PSD-95, ZO-1/-2, and *dlg-A*, which suggests that both intracellular sides of the neuroligin–β-neurexin junction are assembled by similar but distinct PDZ domain proteins. Further interactions of PSD-95 and CASK with other components—for example, NMDA2 receptors and K^+ channels—create the associated structures of the junctions. Thus, an asymmetric junction would be formed in which the junctional proteins recruit associated channels and receptors to the site of the cell-cell interaction by direct protein interactions (Fig. 6).

Does this junction correspond to the synapse? Like synapses, it is asymmetric and contains receptors and channels. Furthermore, PSD-95 is localized to postsynaptic densities (*1*), and neurexins, neuroligins, and CASK are enriched in synapses, although they are not exclusively localized there (*4*, *5*, *14*). Finally, the relatively late peak in expression of neurexins and neuroligins during development suggests a function of mature neurons. On the other hand, an α-neurexin was recently detected in electric rays on axons of the peripheral nerves, although the ultrastructural localization of neurexin was not determined (*15*). Thus we cannot be certain from these data whether the PSD-95–neuroligin–β-neurexin–CASK junction is central to synapses, whether it represents a cell–cell contact at the periphery of synapses like cadherin-mediated junctions (*16*), or whether it is unrelated to synapses—for example, as an intermediate in the biogenesis of synapses. Genetic experiments to address these questions are under way.

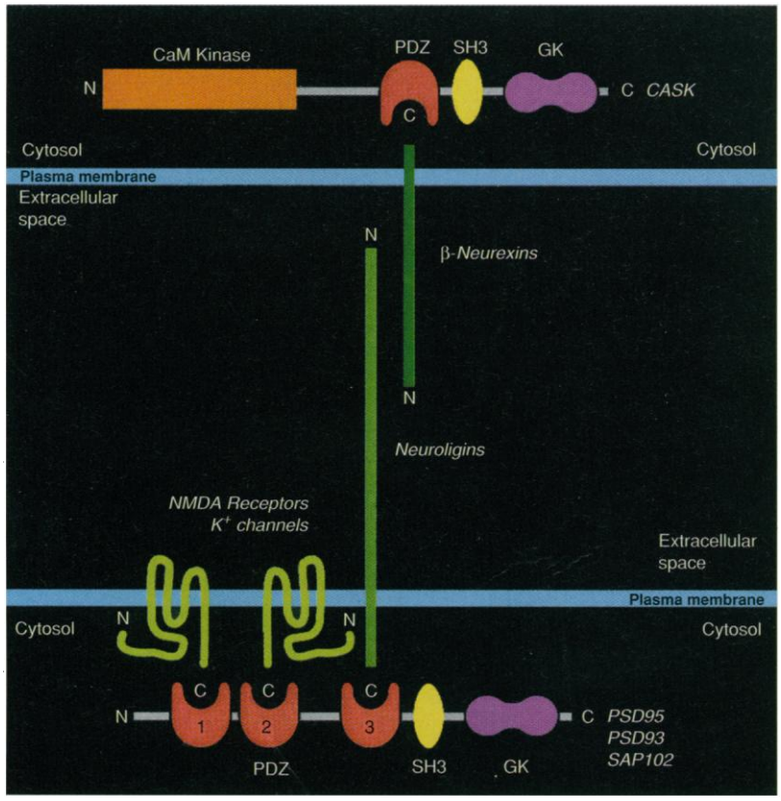

Fig. 6. Model for intercellular junction formation by interactions of PDZ domain proteins with neuroligins and β-neurexins. PSD-95, bound to cytoplasmic tails of neuroligins, and CASK, bound to cytoplasmic tails of β-neurexins, are similarly composed of PDZ, SH3, and guanylate kinase (GK) domains. CASK in addition contains an NH_2-terminal Ca^{2+}-calmodulin–dependent protein kinase module (CaM Kinase). PSD-95 binds to neuroligins via its third PDZ domain and recruits to the junction NMDA2 receptors and K^+ channels that bind to the other PDZ domains. The other domains of CASK and PSD-95 presumably serve to assemble additional, as yet unidentified, junctional components at the interface between the cells.

REFERENCES AND NOTES

1. K. Cho, C. A. Hunt, M. B. Kennedy, *Neuron* **9**, 929 (1992); U. Kistner *et al.*, *J. Biol. Chem.* **268**, 4580 (1993); C. A. Hunt, L. J. Schenker, M. B. Kennedy, *J. Neurosci.* **16**, 1380 (1996); E. Kim, K. Cho, A. Rothschild, M. Sheng, *Neuron* **17**, 103 (1996); B. M. Müller *et al.*, *ibid.*, p. 255.
2. D. F. Woods and P. J. Bryant, *Cell* **66**, 451 (1991); P. Ruff, D. W. Speicher, A. Husain-Chishti, *Proc. Natl. Acad. Sci. U.S.A.* **88**, 6595 (1991); E. Willott *et al.*, *ibid.* **90**, 7834 (1993); D. F. Woods and P. J. Bryant, *J. Cell Sci.* **17**, 171 (1993); L. A. Jesaitis and D. A. Goodenough, *J. Cell Biol.* **124**, 949 (1994).
3. H.-C. Kornau, L. T. Schenker, M. B. Kennedy, P. H. Seeburg, *Science* **269**, 1737 (1995); E. Kim, M. Niethammer, A. Rothschild, Y. N. Jan, M. Sheng, *Nature* **378**, 85 (1995); M. Niethammer, E. Kim, M. Sheng, *J. Neurosci.* **16**, 2157 (1996); L.-F. Lau *et al.*, *J. Biol. Chem.* **271**, 21622 (1996).
4. K. Ichtchenko *et al.*, *Cell* **81**, 435 (1995); K. Ichtchenko, T. Nguyen, T. C. Südhof, *J. Biol. Chem.* **271**, 2676 (1996).
5. Y. A. Ushkaryov, A. G. Petrenko, M. Geppert, T. C. Südhof, *Science* **257**, 50 (1992); Y. A. Ushkaryov and T. C. Südhof, *Proc. Natl. Acad. Sci. U.S.A.* **90**, 6410 (1993); Y. A. Ushkaryov *et al.*, *J. Biol. Chem.* **259**, 11987 (1994); B. Ullrich, Y. A. Ushkaryov, T. C. Südhof, *Neuron* **14**, 497 (1995).
6. T. Nguyen and T. C. Südhof, *J. Biol. Chem.*, in press.
7. Total RNA from forebrain was isolated from mice on postnatal days 0, 2, 5, 7, 10, 12, 15, 20, 30, and 60. RNA blots obtained with formaldehyde gels were hybridized with ^{32}P-labeled probes from neurexins, neuroligins, GAP-43, syntaxin 1, synaptobrevin 2,

and synaptotagmin 1. All blots were hybridized with a GAPDH probe to control for RNA loading. ^{32}P signals were quantified by PhosphorImager detection and are expressed as ratio to GAPDH.

8. A rat brain cDNA library in the yeast-two hybrid prey vector pVP16 [A. B. Vojtek, S. M. Hollenberg, J. A. Cooper, *Cell* **74**, 205 (1993)] was screened as described [S. Fields and O. Song, *Nature* **340**, 245 (1994)] (*14*) with the bait vector pBTM116-NL2-1 (*8*). Of 16 prey clones isolated, pPrey500 encodes residues 1 to 287, and pPrey514 encodes residues 308 to 425 of PSD-95 (*1*). β-Galactosidase assays were corrected for protein concentration [M. D. Rose, F. Winston, P. Hieter, *Methods in Yeast Genetics* (Cold Spring Harbor Laboratory Press, Cold Spring Harbor, NY, 1990); Y. Hata and T. C. Südhof, *J. Biol. Chem.* **270**, 13022 (1995)].
9. The full-length sequence of rat PSD-95 (residues 1 to 724), its NH_2-terminus (residues 1 to 431), and its COOH-terminus (residues 430 to 724) were cloned by PCR with oligonucleotides 1176 (GCGCTCGAGGTACCATGGACTGTCTCTGTATAGTGAC), 1177 (CGCGTCGACTAGAAGCCCCTCTTGGGGTT), 1178 (CGCCTCGAGGAATCAGAGTCTCTCTCGGGC), and 1198 (GCGAATTCTCCATGGGCTTCTACATTAGGGCC). To identify additional members of the PSD-95 family, we used a degenerate PCR strategy. Products from PCRs with redundant oligonucleotide primers complementary to conserved sequences (T73 = TICCI[C,T]A[C,T]ACIACI[C,A]GICC; T75 = AC[G,A]TCIA[G,A]AT[G,A]CA[G,A]TG; T76 = GGIGA[C,T]ATI[C,T]TICA[C,T]GT; I = inosine; brackets = redundant positions) were subcloned and sequenced. We used two products (A290 and A309) containing unusual sequences related to PSD-95 as probes to isolate full-length clones pDLG54 and pDLG70 (GenBank accession numbers U53367 and U53368). The same two isoforms have been independently reported as PSD-93/chapsyn and SAP102 (*1*). pDLG54 is identical with SAP102 except for the absence of the sequence VTSNTSDSESSSKG (residues 627 to 630) (*17*), which suggests that pDLG54 represents a splice variant of SAP102. pDLG70 corresponds to PSD-93/chapsyn with several amino acid differences that may be due to alternative splicing or sequencing variations. The neuroligin bait vectors used encode the following residues of the rat proteins (*4*): pBTM116-NL1-1, 718–843; pBTM116-NL1-2, 718–840; pBTM116-NL1-5, 718–828; pBTM116-NL1-6, 828–843; pBTM116-NL1-10, 796–843; pBTM116-NL2-1, 699–836; pBTM116-NL2-2, 699–786; pBTM116-NL2-3, 786–836; pBTM116-NL3, 730–848. The NMDA2 receptor bait plasmids encode residues 1455–1464 (pBTM116NMDAR2A) and 1473–1482 (pBTM116NMDAR2B) of the rat NMDA-2A and -2B receptors. pBTM116Shaker encodes residues 645–654 of the rabbit Kv1.4 K^+ channel isoform. The different prey vectors are from rat except for ZO-1 (mouse) and *dlg-A* (*Drosophila*) and encode the following residues: PSD-95, pVP16PSD-95-2 = 1–431; pVP16SAP90-5 = 69–150; pVP16SAP90-6 = 160–245. SAP102, pVP16SAP102-1 = 1–519. PSD-93, pVP16PSD-93-1 = 1–539. ZO1, pVP16ZO1-1 = 1–500. *dlg-A*, pVP16dlg-1 = 1–598. Nitric oxide synthase, pVP16NOS = 1–101.
10. D. A. Doyle *et al.*, *Cell* **85**, 1067 (1996).
11. Synthetic peptides were purified on a Kromasil 100 C_{18} reversed-phase column (sequences: NMDAR2A, SNRRVYKKMPSIESDV; NL1-1, LPHPHPHPHSHSTTRV; NL1-2, LPHPHPHPHSHST; control, KFIEAGQYNSHLYGTSV). NMDAR2A and NL1-1 correspond to the COOH-terminus of NMDA2A and neuroligin 1, respectively. NL1-2 is identical with NL1-1 except it lacks the last three amino acids. The control peptide is composed of residues 597 to 613 from PSD-95/SAP90. Peptides were immobilized on a CM5 research grade sensor chip with the amine coupling kit (Pharmacia), equilibrated with 50 mM Hepes-NaOH (pH 8.0) containing 100 mM NaCl, and superfused with GST fusion proteins at different concentrations (flow rate, 20 μl/min). Binding activities (in resonance units) were measured as the difference between the baseline value determined 10 s before sample injection and the measurements taken at the indicated time points. All experiments were performed at 25°C. Data were analyzed with the BIA Evaluation program 2.1 (Pharmacia) [U. Joehnsson *et al.*, *BioTechniques* **11**, 520 (1991)].
12. IgG fusion proteins of the extracellular domains of neurexin 1β with and without an insert in splice site 4 and control IgG fusion protein were purified from transfected COS cells (*4*). Twelve rat brains were homogenized in 48 ml of 20 mM Hepes-NaOH (pH 8.0), 1% (*w/v*) NP-40, 0.2 M NaCl, 2 mM EGTA, and phenylmethylsulfonyl fluoride (0.1 g/liter) in a glass Teflon homogenizer and centrifuged (100,000*g* for 60 min at 4°C). The supernatant (60 ml) was adjected to 3.5 mM $CaCl_2$. Supernatant (20 ml) (0.2 to 0.3 g of protein) was incubated overnight at 4°C with recombinant IgG fusion proteins immobilized on protein A-Sepharose. Beads were washed repeatedly by centrifugation in 20 mM Hepes-NaOH (pH 8.0), 2.5 mM $CaCl_2$, 0.2 M NaCl, and 0.5% NP-40 and eluted sequentially with 0.3 ml of the wash buffer containing 0.5 M NaCl and with 0.5 ml of 20 mM Hepes-NaOH (pH 8.0), 0.1 M NaCl, 10 mM EGTA, and 0.5% NP-40. Fractions were analyzed by SDS–polyacrylamide gel electrophoresis and by immunoblotting with antibodies to PSD-95 (polyclonal antiserum L667 and two independent monoclonal antibodies) and to neuroligin 1 (polyclonal antiserum L067). To exclude the possibility that PSD-95 directly interacts with neurexin 1β, extracts from COS cells transfected with full-length PSD-95 were affinity chromatographed on immobilized neurexin 1β in the absence and presence of recombinant neuroligin.
13. HEK293 cells were transfected with pCMVPSD95-1 encoding full-length rat PSD-95 either alone or together with pCMVNL18, pCMVNR2A, or pCMVNR1 encoding full-length neuroligin 1, NMDA2A, or NMDA1, respectively. Cells were stained with a mouse monoclonal antibody to PSD-95 and rabbit polyclonal antibodies to neuroligin 1 (L067) or the two NMDA receptors (from Chemicon). Images were obtained on a Bio-Rad MRC1024 confocal microscope.
14. Y. Hata, S. Butz, T. C. Südhof, *J. Neurosci.* **16**, 2488 (1996).
15. A. B. Russell and S. S. Carlson, *ibid.* **17**, 4734 (1997).
16. N. Uchida, Y. Honjo, K. R. Johnson, M. J. Wheelock, M. Takeichi, *J. Cell Biol.* **135**, 767.
17. Abbreviations for amino acids are as follows: A, Ala; C, Cys; D, Asp; E, Glu; F, Phe; G, Gly; H, His; I, Ile; K, Lys; L, Leu; M, Met; N, Asn; P, Pro; Q, Gln; R, Arg; S, Ser; T, Thr; V, Val; W, Trp; Y, Tyr.
18. We thank A. Roth, E. Borowicz, and I. Leznicki for excellent technical assistance; M. B. Kennedy (CalTech) for monoclonal antibodies to PSD-95; S. Nakanishi (Kyoto) for NMDA receptor cDNA clones; and M. Missler, M. S. Brown, and J. L. Goldstein for advice. Partially supported by grants from the NIH (RO1-MH52804), the Perot Family Foundation, and the ERATO (Japan Science and Technology Co.). Y.H. was supported by a postdoctoral fellowship from the HFSP, and T.W.R. from the DFG.

10 March 1997; accepted 14 July 1997

Postsynaptic Glutamate Transport at the Climbing Fiber–Purkinje Cell Synapse

Thomas S. Otis,* Michael P. Kavanaugh, Craig E. Jahr

The role of postsynaptic, neuronal glutamate transporters in terminating signals at central excitatory synapses is not known. Stimulation of a climbing fiber input to cerebellar Purkinje cells was shown to generate an anionic current mediated by glutamate transporters. The kinetics of transporter currents were resolved by pulses of glutamate to outside-out membrane patches from Purkinje cells. Comparison of synaptic transporter currents to transporter currents expressed in *Xenopus* oocytes suggests that postsynaptic uptake at the climbing fiber synapse removes at least 22 percent of released glutamate. These neuronal transporter currents arise from synchronous activation of transporters that greatly outnumber activated AMPA receptors.

The glutamate transporters EAAT3 and EAAT4 are expressed at high levels in cerebellar Purkinje cells (PCs) (*1*). Transporters on PCs exhibit substrate-induced anion currents (*2*) similar to those associated with other native (*3*, *4*) and cloned glutamate transporters (*5*–*7*). Because the conductance associated with the glutamate transporter has a high permeability to NO_3^- and SCN^- (*4*, *6*), they were used as the major intracellular anions in PC recordings. Extracellular stimulation in the granule cell layer of cerebellar slices elicited all-or-none excitatory postsynaptic currents (EPSCs), suggesting activation by single climbing fiber (CF) afferents (Fig. 1A) (*8*). These currents were mediated in part by AMPA (α-amino-3-hydroxy-5-methyl-4-isoxazolepropionic acid) receptors, because 10 to 25 μM NBQX blocked more than 95% of the current (Fig. 1A) and addition of the specific AMPA receptor antagonist GYKI 52466 (15 to 25 μM, $n = 3$) or the *N*-methyl-D-aspartate (NMDA) receptor antagonist (±)-3-(2-carboxy piperazin-4-yl)-propyl-1-phosphonic acid (CPP) (2.5 μM) caused no further inhibition. After blockade of AMPA and NMDA receptors, stimulation still activated inward currents with NO_3^- (Fig. 1B) ($n = 25$) or SCN^- ($n = 6$) but not with Cl^-- (Fig. 1B, inset) ($n = 3$) or gluconate-based ($n = 3$) pipette solutions.

Vollum Institute, L-474, Oregon Health Sciences University, 3181 Southwest Sam Jackson Park Road, Portland, OR 97201, USA.

*To whom correspondence should be addressed.